

## Chapter 7 Recrystallisation after cold work of low carbon Al-killed strip steels

---

### 7.1 Introduction

The annealing of cold worked Al-killed steels has been a subject of many investigations<sup>(8-11,60,122-124)</sup>. These studies have been concerned with the kinetics of recrystallisation, with microstructure and texture development and with the individual and combined effects of composition, thermal history prior to cold work and heating rates during subsequent annealing.

The extent of isothermal recrystallisation with time follows the normal sigmoidal relationship and is mostly modelled by the JMAK equation. This is with the exception in some cases of Al-killed steels where the process is inhibited by the precipitation of AlN precipitates.

### 7.2 Interaction between AlN precipitation and the recrystallisation process after cold work

The greatest limitation in the study of the interaction between the precipitation of AlN and the recrystallisation process in low carbon Al-killed strip steels has been the difficulty in observing the very early stages of AlN precipitation in deformed structures by electron microscopy. Meyzaud et al<sup>(8)</sup> studied the precipitation of AlN indirectly by the electrical resistivity method, see figure 7.1.

## Chapter 7 Recrystallisation after cold work of low carbon Al-killed strip steels

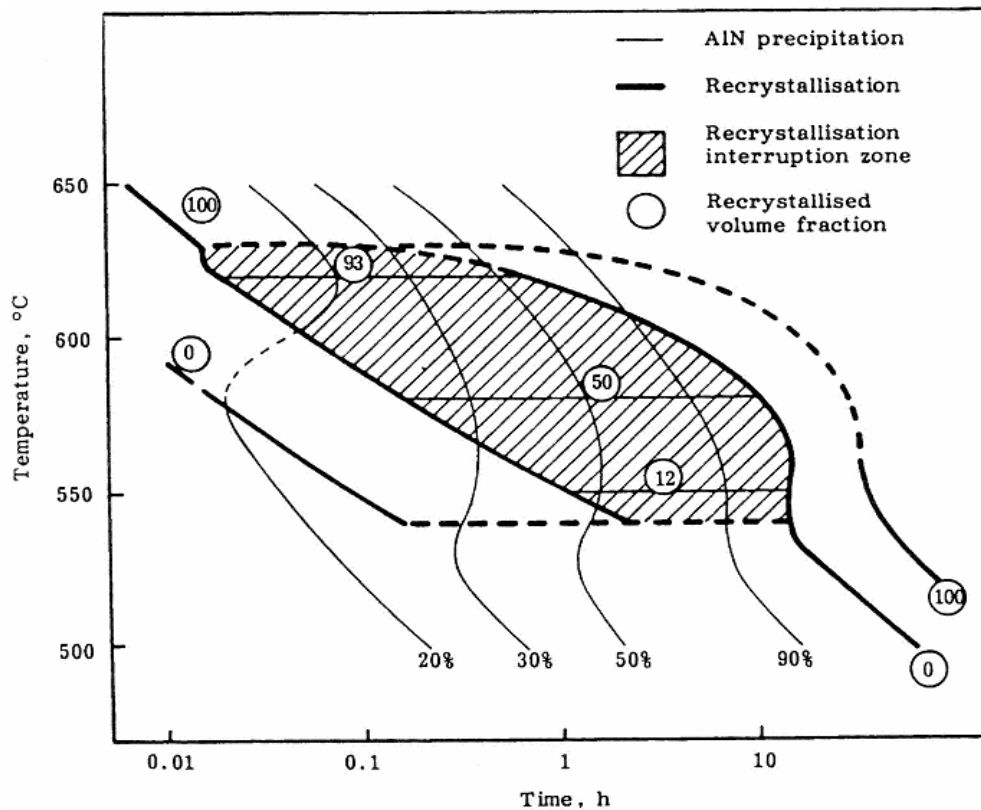


**Figure 7.1:** The TTT curves for recrystallisation and AlN precipitation in cold rolled (70 percent deformation) Al-killed steel<sup>(8)</sup>.

The interaction between AlN precipitation and recrystallisation can be described as follows: at higher temperatures ( $> 650\text{ }^{\circ}\text{C}$ ), recrystallisation precedes precipitation, at lower temperatures ( $< 550\text{ }^{\circ}\text{C}$ ) precipitation precedes recrystallisation, while at intermediate temperatures both proceed together. However, at these intermediate temperatures, the recrystallisation process is retarded and only accelerates again after growth and coarsening of the AlN precipitates has made their pinning force ineffective. This observation agrees with earlier studies on the effect of solute

## Chapter 7 Recrystallisation after cold work of low carbon Al-killed strip steels

---

atoms and their subsequent precipitation on the recrystallisation process<sup>(8-11,92,112)</sup>. It has been observed that in Al-killed steels and during isothermal annealing after cold work, the recrystallisation process is inhibited by the nucleation/clustering of AlN on subgrain boundaries and dislocations. Goodenow et al<sup>(118)</sup> observed that during isothermal annealing at 580 °C after cold work, recrystallisation took place at shorter times in rimmed steels than in Al-killed steels and it was suggested that this was caused by the “precipitation/clustering” of AlN. As mentioned earlier, the greatest challenge has always been the failure to observe the pinning effect directly by electron microscopy on the recrystallisation process in the early stages of the clustering/precipitation of the AlN. Nevertheless, this effect has been used with relative success in microstructure and texture control during annealing after cold work in these steels.

### 7.3 Influence of S, Mn and MnS on the recrystallisation process after cold work

In a study<sup>(119)</sup> on the influence of sulphur in solid solution on static recrystallisation of cold worked low carbon manganese strip steels, it was found that increasing the content of sulphur in solid solution in the steel, retarded the recrystallisation process, see figure 7.2. As may be seen, the increase in sulphur in solid solution did not only increase the incubation period for recrystallisation but also resulted in only partial recrystallisation of the steel. It was suggested that the sulphur or both the sulphur and manganese, inhibit the nucleation and growth of new grains

## Chapter 7 Recrystallisation after cold work of low carbon Al-killed strip steels

by segregating to the grain boundaries. Prior annealing of the steel at 700 °C to precipitate the MnS before cold work, increased the recrystallisation kinetics as shown in figure 7.2, with the top curve for the steel with less than 10 ppm sulphur in solid solution, recrystallising faster. Although their results were not conclusive, Baird et al<sup>(120)</sup> made similar observations earlier that sufficient amount of sulphur in solid solution (50 ppm) gave rise to difficulty in recrystallisation of iron. Their evidence was based on the fact that when manganese was added to the iron to form MnS, the iron recrystallised normally without exhibiting any “sluggish” behaviour.

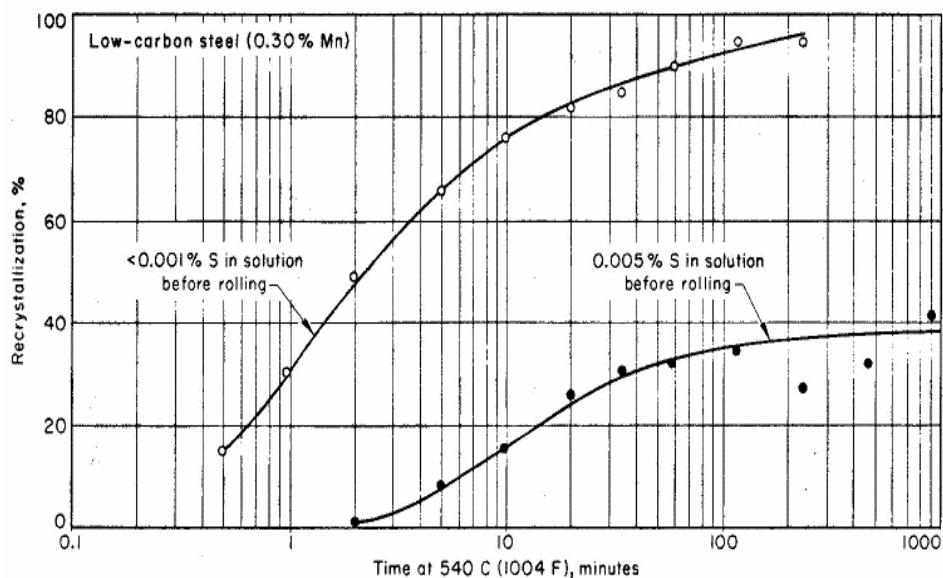


Figure 7.2: Effect of annealing time at 540 °C on the percentage of recrystallisation in 60 percent cold worked low carbon manganese strip steels containing two different amounts of S in solid solution before cold rolling. Note the retarded recrystallisation of the steel with more S in solid solution<sup>(119)</sup>.

## Chapter 7 Recrystallisation after cold work of low carbon Al-killed strip steels

---

In another study<sup>(122)</sup> on the influence of solute manganese on static recrystallisation of cold worked Al-killed steels with 70 ppm sulphur, it was found that increasing the solute content of manganese, retarded the recrystallisation process by increasing the incubation period without affecting the nucleation and growth rate of the recrystallisation, see figure 7.3. It was proposed that the prolonged incubation period was probably not directly as a result of the solute manganese as such but rather as a result of Mn-C complexes that had strong interaction with dislocations.

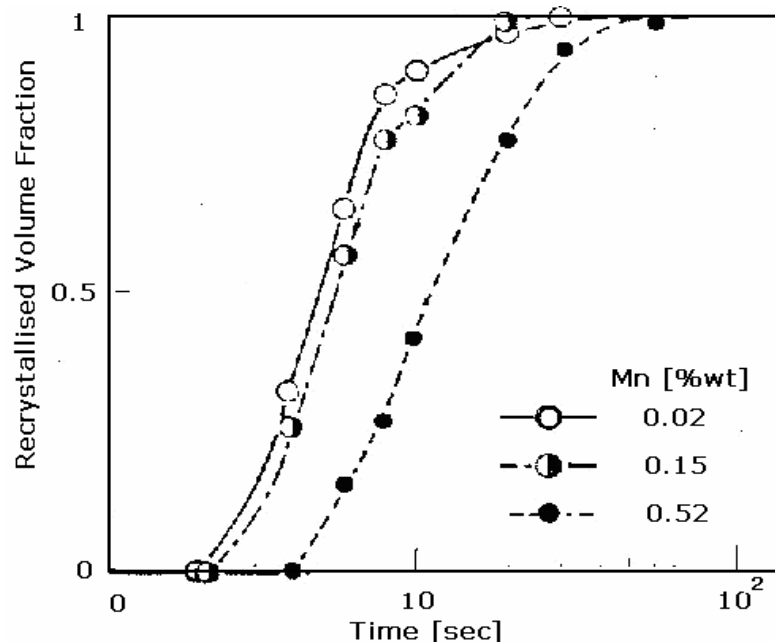


Figure 7.3: Influence of solute Mn on the recrystallisation progress in 80 percent cold worked Al-killed low carbon-manganese steel during isothermal annealing at 650 °C<sup>(122)</sup>

## Chapter 7 Recrystallisation after cold work of low carbon Al-killed strip steels

---

Frawley et al<sup>(68)</sup> also observed in high sulphur low carbon steels that the finer MnS with a diameter of 5 to 30 nm, and or the sulphur in solid solution, retarded the dynamic recrystallisation of austenite during laboratory hot rolling in thin slab direct rolling (TSDR), i.e. in a simulated HCR experiment. However this study did not separate the effect of sulphur from that of MnS on the dynamic recrystallisation process in these steels.

## Chapter 8 Techniques to determine the solubility of AlN and free nitrogen in Al-killed low carbon strip steels

---

### 8.1 Introduction

Methods of measuring free nitrogen in steels may be direct or indirect. Some of the direct techniques include chemical analysis and hot hydrogen extraction while the indirect techniques, include the strain ageing index method, thermoelectric power techniques (TEP), resistivity techniques, magnetic techniques and internal friction. Some of these techniques are discussed briefly in the following sections.

### 8.2 Chemical analysis

The iron matrix is dissolved without dissolving the aluminium nitride and the insoluble nitrides are then separated through filtration. The most common used chemical dissolution technique for separating AlN from the iron matrix is that developed by Beeghly<sup>(53)</sup>. Although the Beeghly technique was criticized for lack of sensitivity to small particles of less than 10 nm in size and failure to isolate the AlN from other nitrides, it is still widely used in the determination of free nitrogen in low carbon steels<sup>(66)</sup>.

### 8.3 Hot hydrogen extraction method

The use of hydrogen to combine with free nitrogen in a steel in a hydrogen furnace at about 500 °C, is one of the oldest techniques that is still used today to determine the free nitrogen content in steels. The diffusivity and solubility of both nitrogen and hydrogen at the test temperature need to be established in order to determine the annealing time that would ensure adequate

## Chapter 8 Techniques to determine the solubility of AlN and free nitrogen in Al-killed low carbon strip steels

---

diffusion of hydrogen into the steel, taking into account the sample size and temperature. Fine metal shavings are preferred as this ensures efficient combination of the hydrogen and nitrogen through shorter diffusion paths.

The hydrogen also accelerates the rate of escape of nitrogen by reducing the oxide layer that may form on the surface of the metal and inhibit the escape of nitrogen. Hydrogen combines with the free nitrogen on the surface in a suggested sequence as follows<sup>(53)</sup>:



The captured ammonium gas is then quantitatively analysed by conventional chemical analysis techniques.



## Chapter 8 Techniques to determine the solubility of AlN and free nitrogen in Al-killed low carbon strip steels

---

### 8.4 Strain aging index method

Free carbon and nitrogen atoms fill the interstitial positions of the iron crystal lattice, creating strain within the lattice structure due to the atom misfit. As a result, these interstitial atoms segregate to dislocations in order to lower the system's strain energy. Since the interstitial voids for austenite (fcc) are greater than that for ferrite (bcc), the driving force for segregation to dislocations is less in austenite than in ferrite. These interstitial atoms form a cloud of atoms or "Cottrell atmospheres" on the dislocations, locking the glissile ones in the process. This phenomenon has a strengthening effect that is reflected in the increase in yield strength of the material and, therefore, can be used indirectly to measure the content of interstitial solutes. This technique is generally called the "strain aging index method" and is preferred to the other techniques for its simplicity, see figure 8.1. However, as may be seen in figures 8.2 and 8.3, one should be mindful of the large scatter in results associated with this technique. Morrison et al<sup>(126)</sup> correlated the increase in yield strength  $\Delta Y$  to the free nitrogen content as shown in figure 8.2.

## Chapter 8 Techniques to determine the solubility of AlN and free nitrogen in Al-killed low carbon strip steels

---

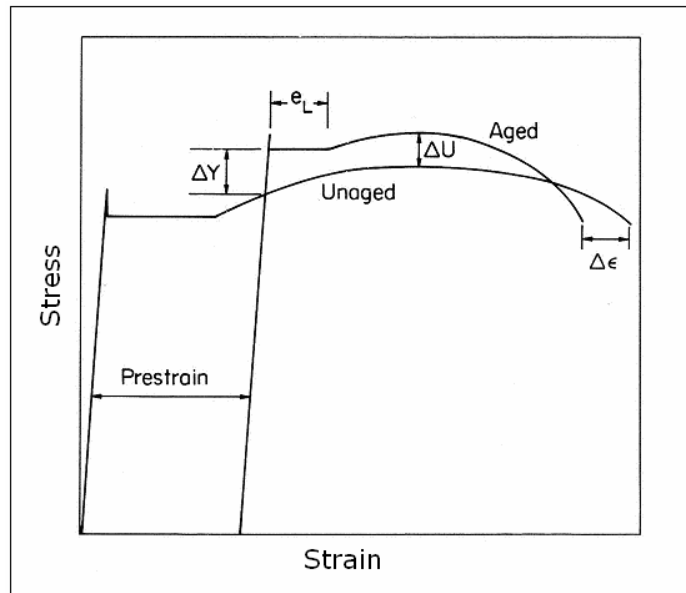


**Figure 8.1: Effect of static aging on the load-elongation curve of iron containing interstitial solutes:  $\Delta Y$  = change in yield stress due strains aging,  $e_L$  = Lüder's strain after strain aging,  $\Delta U$  = increase in ultimate tensile strength and  $\Delta \epsilon$  = decrease in elongation due to strain aging<sup>(125)</sup>.**

The diffusivity of nitrogen at low temperatures ( $<400\text{ }^\circ\text{C}$ ) is higher than that of carbon and, therefore, in the absence of aluminium in the steel, strain aging is mainly caused by nitrogen. At temperatures below  $100\text{ }^\circ\text{C}$ , the effect of nitrogen is about twice that of carbon<sup>(127)</sup> (see figure 8.3). As may be seen, solute nitrogen at levels as low as 5 ppm, would give an increase of about 20 MPa in yield strength.

## Chapter 8 Techniques to determine the solubility of AlN and free nitrogen in Al-killed low carbon strip steels

---

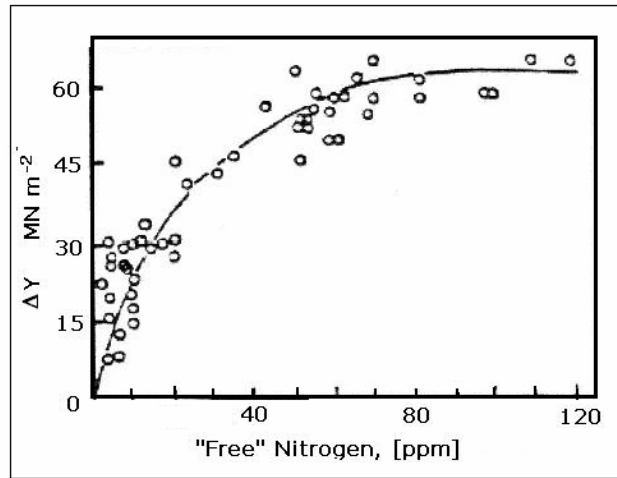


Figure 8.2: Influence of free nitrogen content on the magnitude of strain aging in low carbon sheet steels, (Morrison et al<sup>(126)</sup>).

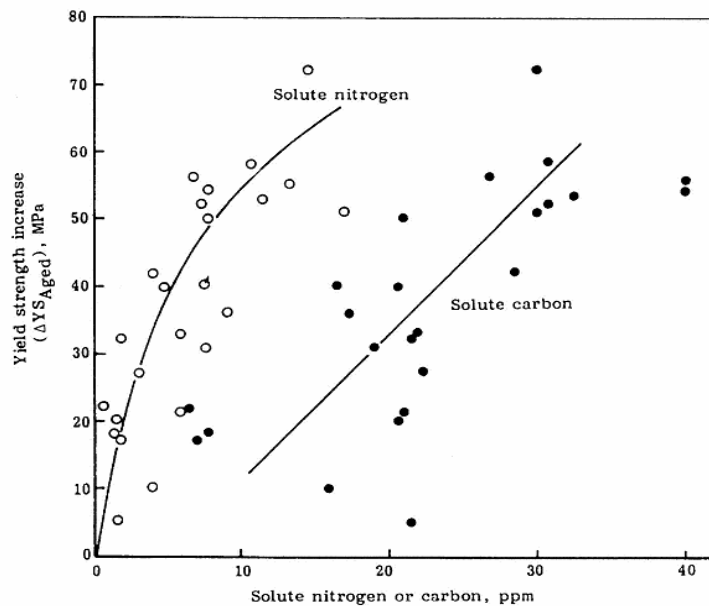


Figure 8.3: Influence of C and N on the yield strength of a low carbon and aluminium-killed steel after 70 percent cold reduction and aging at 38 °C for 30 days<sup>(127)</sup>.

## Chapter 8 Techniques to determine the solubility of AlN and free nitrogen in Al-killed low carbon strip steels

---

### 8.5 Internal friction methods (Snoek effect)

The redistribution of interstitial atoms (C and N) following elastic lattice distortion, causes the strain to lag behind the stress. This behaviour is also known as the Snoek effect, after its discoverer<sup>(128)</sup>. When a crystal is elastically stretched in the  $z$ -direction then there is a preference for the interstitial atoms to occupy the elongated  $z$  sites and a shift in the equilibrium positions occurs, such that the number of occupied  $z$  (octahedral or tetrahedral) sites increases whilst those sited in the  $x$  and  $y$  axis directions decrease. This redistribution of interstitial atoms takes a little while upon instantaneous application and removal of stress. The rate at which this happens is determined by the frequency of jumping of these atoms and consequently by the temperature. The characteristics of the jump frequency are unique to particular interstitial atoms and, therefore it is possible to separate the effects of nitrogen from those of carbon, at least in principle.

The maximum internal friction is attained when the period of application of stress equals the jump time. The Snoek effect is usually observed through free torsional oscillations of the sample and its peak is proportional to the concentration of the interstitial atoms in solid solution.

The interstitial solutes that contribute to internal friction in the manner described above are those that occupy the normal sites in the undistorted lattice. Atoms within the strain field of a

## Chapter 8 Techniques to determine the solubility of AlN and free nitrogen in Al-killed low carbon strip steels

---

dislocation, those neighbouring a substitutional solute atom, or those at grain boundaries will not react in the same way to the applied stress<sup>(129)</sup>. For this reason, internal friction measurements have not been successfully used in determining the carbon and nitrogen concentrations in solid solution of commercial steels.

### 8.6 Thermoelectric power (TEP) method (Seebeck effect)

The TEP technique is based on the phenomenon called the Seebeck effect<sup>(130)</sup>, named after its discoverer in 1822. This effect occurs because at the hot junction, the Fermi energy of the electrons is higher than at the cold junction. The higher energy electrons at the hot end lower their energy by diffusing to the cold junction. Consequently the cold junction becomes negatively charged and the hot junction positively charged and a voltage drop is induced between the two junctions. This technique is applicable to materials that conduct electricity.

The TEP is a proportionality coefficient between the electron flux (emf) and the temperature gradient  $\Delta T$  that exists between the cold and hot junctions of the test sample, as illustrated in figure 8.4. The TEP is affected by lattice defects and is the sum of various contributions i.e.

$$\Delta S = \Delta S_{ss} + \Delta S_d + \Delta S_{pp} \quad (8.5)$$

## Chapter 8 Techniques to determine the solubility of AlN and free nitrogen in Al-killed low carbon strip steels

---

where  $\Delta S_{ss}$ ,  $\Delta S_d$ , and  $\Delta S_{pp}$  are due to the elements in solid solution, dislocations and precipitates respectively

The TEP measurement between the test specimen and the reference specimen is given by:

$$\Delta S = \frac{\Delta V}{\Delta T} = S - S_0 \quad (8.6)$$

where  $\Delta V$  is the emf difference between the test specimen and the reference specimen,  $\Delta T$  is the temperature difference between the cold and hot junctions of both the test specimen and the reference,  $S$  and  $S_0$  are the absolute TEP values of the test specimen and the reference respectively.

When using the Seebeck effect to analyse the chemical composition of a metal, two distinct phenomena may affect the TEP: the diffusion of electrons through the test metal and the phonon drag. If a temperature gradient exists across the conductor, phonons (thermal lattice vibrations) will move from the hot to the cold junction against the flow of electrons causing, what is known as phonon drag. This phenomenon is significant at temperatures below twenty percent of the Debye temperature<sup>(131-134)</sup>. It is, therefore, important that the TEP measurements are carried out above the twenty percent level of the Debye temperature of iron, which is 477 K, where the diffusion of electrons dominates over phonon drag in order to separate the two effects. Measurements at and around 0°C to room

## Chapter 8 Techniques to determine the solubility of AlN and free nitrogen in Al-killed low carbon strip steels

---

temperature are, therefore, adequate to separate these two effects.

### 8.6.1 Effect of solid solution on the TEP

For concentrations of  $<0.1$  at% of an element in solid solution, the TEP decreases proportionally with the increase in concentration of the element in solid solution, as illustrated in figure 8.4. It is worthwhile to note that a concentration  $>0.1$  at% results in interactions between the solute atoms themselves and, therefore, this affects the Gorter-Nordheim linear relationship between the TEP and the concentration of the solute atoms, equation 8.7.

The slope of the graph of the TEP versus the concentration of the element in solid solution, gives the proportionality constant known as the TEP coefficient, see figure 8.5. This is represented by the Gorter-Nordheim law<sup>(135)</sup>, which is expressed as follows:

$$\Delta S_{ss} = K_i \cdot [i]_{ss} \quad (8.7)$$

where  $[i]_{ss}$  represents the content of the solute element and  $K_i$  is the TEP coefficient of the element.

## Chapter 8 Techniques to determine the solubility of AlN and free nitrogen in Al-killed low carbon strip steels

---

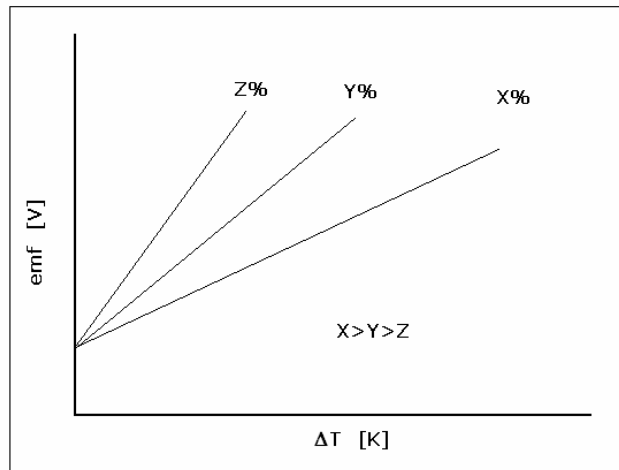


Figure 8.4: Schematic graph showing variation of emf with change in temperature. The slopes are the TEP values for the solute element in different concentrations X, Y and Z, with all concentrations  $< 0.1$  at%.

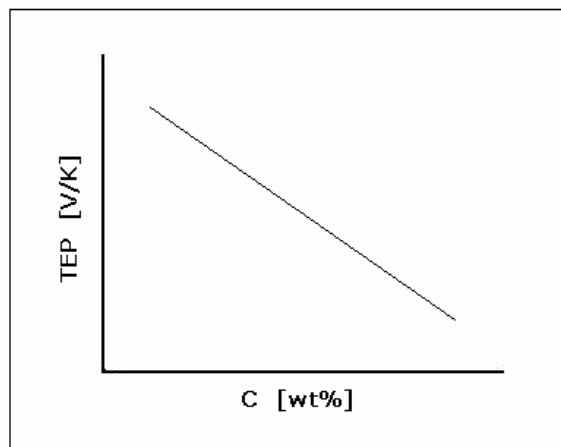


Figure 8.5: Schematic diagram of TEP versus content of the element in solid solution and the slope of this graph is the TEP coefficient of the latter.



## Chapter 8 Techniques to determine the solubility of AlN and free nitrogen in Al-killed low carbon strip steels

---

### 8.6.2 Effect of dislocations and precipitates on TEP measurements

It has been observed<sup>(136)</sup> that cold working has a negative effect on the TEP just the same as adding solute atoms to the matrix. It is worth noting that solute atoms that segregate to dislocations and grain boundaries and thereby relieve their strain energies in the matrix, do not contribute to the TEP. It is for this reason that measuring of nitrogen in solid solution using this technique, has to be done immediately after quenching from the solution temperature or on samples that are stored in liquid nitrogen in order to avoid strain aging. The contribution of precipitates on the TEP is negligible unless they are small and coherent.

## Chapter 9 Techniques for measuring recrystallised volume fraction in metals

---

### 9.1 Introduction

There are direct and indirect methods of measuring the volume fraction of the recrystallised material. Some of the techniques are discussed in the following sections.

### 9.2 Hardness test

This is the easiest and quickest technique of estimating the volume fraction of the recrystallised material. The amount of recrystallisation is related to the drop in hardness as the annealing time is extended and the volume fraction of the recrystallised material  $X$  is given proportionally as<sup>(137)</sup>:

$$X = \frac{h_o - h_i}{h_o - h_f} \quad (9.1)$$

where  $h_o$  is the microhardness at the start of recrystallisation, (generally measured at the 5% recrystallised state taken as a datum point to avoid the effects of recovery<sup>(137)</sup>),  $h_i$  is the microhardness after annealing for a time  $t_i$  and  $h_f$  is the microhardness in the fully recrystallised state.

As this method assumes a linear or direct relationship of hardness with volume fraction recrystallised (which is not always the case), it is necessary to authenticate the recrystallised volume fraction with metallographic analysis although the 5% recrystallisation volume fraction may not be easy to measure accurately.

## Chapter 9 Techniques for measuring recrystallised volume fraction in metals

In isothermal annealing of cold worked nickel (fcc) and aluminium (fcc), it was observed that hardness was not significantly affected by the recovery process but only by the recrystallisation process<sup>(138,139)</sup>, see figure 9.1. This technique has also been successfully applied to the study of the recrystallisation process in low carbon steels (bcc)<sup>(140)</sup>.

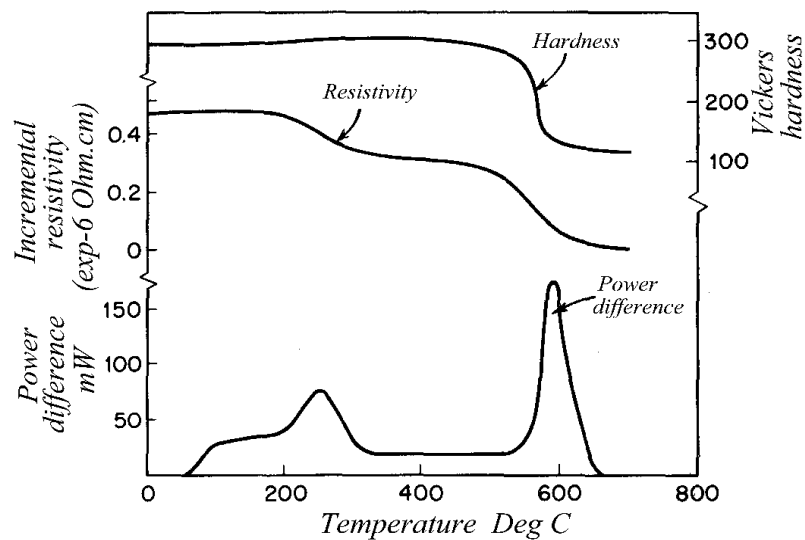


Figure 9.1: Isothermal annealing curves for cold worked nickel (fcc)<sup>(138)</sup>.

Note that both the calorimetry and resistivity techniques are sensitive enough to register both the recovery and recrystallisation peaks whereas the hardness test registers only recrystallisation<sup>(138)</sup>.

### 9.3 Metallographic analysis

This is a widely used technique whereby the material is polished and etched and observed by optical microscopy. The recrystallisation volume fraction is measured by the point count method or through

## Chapter 9 Techniques for measuring recrystallised volume fraction in metals

---

the use of computer software that computes the volume fraction through area fraction analysis from the phase contrast between the recrystallised and non-recrystallised regions of the material. These metallographic techniques are based on the equivalence between the volume fraction and the intercepted area, line or point fractions in opaque two-dimensional material. This principle is well documented in the literature<sup>(141)</sup>. This method, if a reliable phase contrast can be obtained by etching, is preferred as it provides a direct measurement of the volume fraction  $X$  of recrystallised material and is not an indirect one as with hardness measurements.

### 9.4 Electrical resistivity method

Plastic deformation increases the electrical resistivity of the deformed material slightly. This phenomenon is used to indirectly measure the degree of recovery and recrystallisation during the annealing process, provided there is no other phase change taking place simultaneously. One of the weaknesses of this technique is that it is sensitive to specimen size and, therefore, it is imperative to ensure that the different resistivity measurements take into account differences in specimen size.

### 9.5 Differential Scanning Calorimeter

When a piece of metal is plastically deformed, part of the expended energy in the deformation process is retained as stored energy that is later on released in the form of heat during subsequent annealing. The released heat is used to measure the extent of the recrystallisation process. A well annealed reference

## Chapter 9 Techniques for measuring recrystallised volume fraction in metals

---

specimen of the same material as the plastically deformed one and in which no recrystallisation is taking place, is normally used.

Non-isothermal experiments are easier to set up as both the sample and the reference are heated up at the same rate<sup>(142)</sup>. The heat flux  $\dot{E}$  or  $(dE/dt)$ , is measured as a function of temperature  $T$  and the heating rate  $\beta$  is the measuring parameter. As the sample releases the stored energy, less heat is required to maintain the heating rate. The  $\dot{E}_{(T, \beta)}$  heat flux curves often have a peak more or less bell-shaped, figure 8.1, and the total energy  $E_{(T, \beta)}$  released is obtained by integrating the area under the curve within the specified temperature limits. The recrystallised volume fraction can be derived in energy terms<sup>(143)</sup>:

$$X_{(T, \beta)} = \frac{E_{(T, \beta)}}{E_{stored}} \quad (9.2)$$

where  $E_{stored}$  is the energy released in a fully recrystallised material.

The advantage of this technique is that during the annealing process, it is quite common to observe two energy peaks, one for recovery and the other for recrystallisation. This makes it possible to separate the two processes.

## Chapter 9 Techniques for measuring recrystallised volume fraction in metals

---

### 9.6 Electron Back Scattering Diffraction (EBSD)

The electron back scattering diffraction (EBSD) technique is one of the modern techniques that are used to study the recrystallisation process by determining crystal orientation mapping (COM). The grain boundaries are characterised by the orientation relationship between adjacent regions, the grains and subgrains are displayed in a colour code according to their orientation relationships as defined in the software program. The recrystallisation process may be studied through the observation of the number of HAGB i.e. angles above about  $10^\circ$  to  $15^\circ$ .

One weakness with this technique is that it is time consuming when it is required to investigate an area that would be a fair representation of the bulk. In these instances, a compromise between the scanning step size (nm) and the precision of the information to be extracted has to be made.